

THE DIRECT PREDICTION OF BUCKLING LOADS OF SHELLS UNDER AXIAL COMPRESSION USING VCT - TOWARDS AN UPGRADED APPROACH

E.L. Jansen* , H. Abramovich , R. Rolfes***

***Institute of Structural Analysis, Leibniz Universitaet Hannover, Hannover, Germany, ** Faculty of Aerospace Engineering, Technion, I.I.T., Haifa, Israel**

Keywords: Structures, buckling, vibration, nondestructive testing

Abstract

The availability of a Vibration Correlation Technique (VCT) for nondestructive determination of buckling loads of cylindrical shells has obvious advantages. Earlier, a semi-empirical VCT approach has been developed and applied successfully for the prediction of the buckling load of closely stiffened aluminum shells. In the present paper, a possibility to support and improve the estimates of this semi-empirical VCT approach by means of the application of analysis tools is proposed. Two semi-analytical models with different levels of complexity will be used for this purpose. In the two approaches employed, both the nonlinear effect of the static state and the nonlinear effect of the geometric imperfections are represented. These two methods form the basis of an extension of the existing semi-empirical Vibration Correlation Technique for shells, to a VCT in which vibration measurements and analysis tools are combined. In this paper, the capability of the analysis tools which can be used to improve the VCT is illustrated.

1 Introduction

While vibration correlation techniques have been applied to columns and plates for decades and some of them became nearly a routine, the methods developed for shells have not yet entered general use, though their potential benefit exceeds that for other structural elements [1, 2]. Many theoretical studies investigated the influ-

ence of boundary conditions, load eccentricity and geometric initial imperfections of stiffened and unstiffened shells on their vibrational behavior. Based on those theoretical considerations, practical vibration correlation techniques (VCT) have been developed for shells. A detailed review of the VCT approach can be found in Chapter 15 of [2]. The VCT for shells can be classified in two main groups according to their approach: (1) those for determination of boundary conditions, and (2) those for direct determination of buckling loads. The present manuscript will deal solely with the direct nondestructive determination of buckling loads of cylindrical shells.

In the present paper, a possibility to improve the buckling estimates of the empirical VCT methods by means of the use of analysis tools is proposed. Two semi-analytical models with different levels of complexity, which have been developed earlier to analyze the vibration behavior of orthotropic (ring- and stringer-stiffened) and anisotropic (such as composite) cylindrical shells, will be used for this purpose. With these models the influence of important parameters, such as large amplitudes, geometric imperfections, static loading, and boundary conditions on the vibration behavior of cylindrical shells can be investigated. Nonlinear Donnell-type governing equations are adopted in combination with classical lamination theory and smeared stiffener theory. It is assumed that the cylindrical shell is statically loaded by axial compression, radial pressure, and torsion. In the Level-1 Analysis

(or Simplified Analysis) a small number of assumed modes which approximately satisfy simply supported boundary conditions at the shell edges, are used in a Galerkin procedure or variational method. In the Level-2 Analysis (or Extended Analysis) the specified boundary conditions are accurately satisfied by means of the numerical solution of corresponding two-point boundary value problems for ordinary differential equations. In order to apply these analysis tools, equivalent imperfection amplitudes should be determined or assumed. In the methods employed, both the nonlinear effect of the static state and the nonlinear effect of the geometric imperfections are represented. These methods form the basis of an extension of the semiempirical Vibration Correlation Technique for shells, to a VCT in which vibration measurements and analysis tools are combined. In this paper, the capability of the analysis tools which can be used to improve the VCT is illustrated.

In [3] several analytical-numerical models with different levels of accuracy and complexity (denoted as Level-1 and Level-2 Analysis) have been presented which can be used to study the influence of important parameters on shell vibrations, such as geometric imperfections, static loading (axial compression, radial pressure and torsion) and boundary conditions. Nonlinear Donnell-type governing equations are adopted in combination with classical lamination theory. In [3], these models have been compared for the nonlinear vibration analysis of isotropic and orthotropic shells. In [4] laminated shells were studied, while in [5] the effect of imperfections on the linearized vibrations of shells was investigated, and in [6] the effect of boundary conditions on the nonlinear vibrations. In the next section, the underlying theory and analysis models earlier described in [3] and [7] will first be recapitulated.

2 Semi-analytical models for vibrations of statically loaded imperfect cylindrical shells

The shell geometry and the applied loading are defined in Fig. 1. The shell geometry is char-

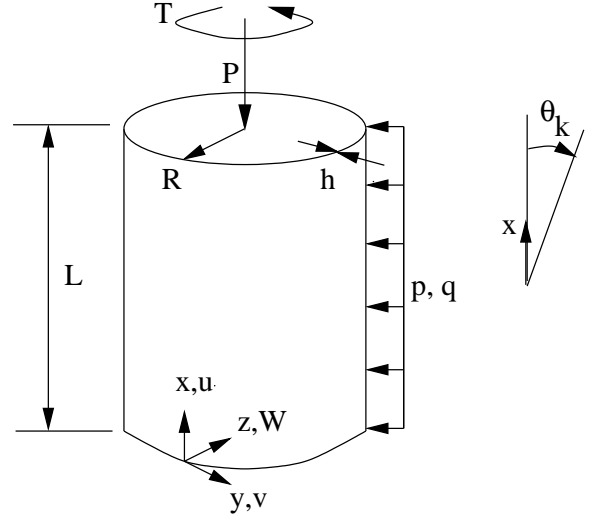


Fig. 1 Shell geometry, coordinate system and applied loading.

acterized by its length L , radius R and thickness h . Assuming that the radial displacement W is positive inward (see Fig. 1) and introducing an Airy stress function F as $N_x = F_{,yy}$, $N_y = F_{,xx}$ and $N_{xy} = -F_{,xy}$, where N_x , N_y and N_{xy} are the usual stress resultants, then the Donnell-type nonlinear imperfect shell equations (neglecting in-plane inertia) for a general anisotropic material can be written as

$$L_{A^*}(F) - L_{B^*}(W) = -\frac{1}{R}W_{,xx} - \frac{1}{2}L_{NL}(W, W + 2\bar{W}) \quad (1)$$

$$L_{B^*}(F) + L_{D^*}(W) = \frac{1}{R}F_{,xx} + L_{NL}(F, W + \bar{W}) + p - \bar{\rho}hW_{,tt} \quad (2)$$

where the variables W and F depend on the time t , R is the shell radius, \bar{W} is an initial radial imperfection, $\bar{\rho}$ is the (averaged) specific mass of the laminate, h is the (reference) shell thickness, p is the (effective) radial pressure (positive inward), and $\bar{\rho}hW_{,tt}$ is the radial inertia term. The fourth-order linear differential operators

$$L_{A^*}(\cdot) = A_{22}^*(\cdot)_{,xxxx} - 2A_{26}^*(\cdot)_{,xxxy} + (2A_{12}^* + A_{66}^*)(\cdot)_{,xxyy} - 2A_{16}^*(\cdot)_{,xyyy} + A_{11}^*(\cdot)_{,yyyy} \quad (3)$$

$$L_{B^*}(\cdot) = B_{21}^*(\cdot)_{,xxxx} + (2B_{26}^* - B_{61}^*)(\cdot)_{,xxxy} + (B_{11}^* + B_{22}^* - 2B_{66}^*)(\cdot)_{,xxyy} + (2B_{16}^* - B_{62}^*)(\cdot)_{,xyyy} + B_{12}^*(\cdot)_{,yyyy} \quad (4)$$

$$L_{D^*}(\cdot) = D_{11}^*(\cdot)_{,xxxx} + 4D_{16}^*(\cdot)_{,xxxy} + 2(D_{12}^* + 2D_{66}^*)(\cdot)_{,xxyy} + 4D_{26}^*(\cdot)_{,xyyy} + D_{22}^*(\cdot)_{,yyyy} \quad (5)$$

depend on the stiffness properties of the laminate. The stiffness parameters A_{ij}^* , B_{ij}^* , and D_{ij}^* are coefficients of the partially inverted ABD-matrix from classical lamination theory and can be found in [3]. The nonlinear operator defined by

$$L_{NL}(S, T) = S_{,xx} T_{,yy} - 2S_{,xy} T_{,xy} + S_{,yy} T_{,xx} \quad (6)$$

reflects the geometric nonlinearity.

The shell can be loaded by axial compression P , radial pressure p and counter-clockwise torsion T (Fig. 1), both statically (\tilde{P} , \tilde{p} , \tilde{T}) and dynamically (\hat{P} , \hat{p} , \hat{T}). The equations governing the nonlinear dynamic behaviour of a cylindrical shell vibrating about a nonlinear static state will be derived, by expressing both the displacement W and the stress function F as a superposition of two states,

$$W = \tilde{W} + \hat{W} \quad (7)$$

$$F = \tilde{F} + \hat{F} \quad (8)$$

where \tilde{W} and \tilde{F} are the radial displacement and stress function of the static, geometrically nonlinear state which develops under the application of a static load on the imperfect shell, while \hat{W} and \hat{F} are the radial displacement and stress function of the dynamic state corresponding to the large amplitude vibration about the static state.

The Donnell-type equations governing the nonlinear dynamic state can be written as

$$L_{A^*}(\hat{F}) - L_{B^*}(\hat{W}) = -\frac{1}{R}\hat{W}_{,xx} - \frac{1}{2}L_{NL}(\tilde{W}, \hat{W}) - \frac{1}{2}L_{NL}(\hat{W}, \tilde{W} + 2\bar{W}) - \frac{1}{2}L_{NL}(\hat{W}, \hat{W}) \quad (9)$$

$$L_{B^*}(\hat{F}) + L_{D^*}(\hat{W}) = \frac{1}{R}\hat{F}_{,xx} + L_{NL}(\tilde{F}, \hat{W}) + L_{NL}(\hat{F}, \tilde{W} + \bar{W}) + L_{NL}(\hat{F}, \hat{W}) + \hat{p} - \bar{\rho}h\hat{W}_{,tt} \quad (10)$$

where \hat{p} is the dynamic radial loading. It is noted that the coefficients of the dynamic state equations depend on the solution of the static state problem.

The Donnell-type equations for the nonlinear dynamic state of a perfect shell can be deduced from Eqs. (9) and (10) [3].

2.1 Simplified Analysis

At the modelling level denoted as Level-1 Analysis or Simplified Analysis, the vibration behaviour is modelled via a Galerkin procedure or variational method. The Level-1 model that will be used to investigate the nonlinear vibrations of statically loaded, imperfect laminated (anisotropic) cylindrical shells is characterized by the following deflection function,

$$\hat{W}(t)/h = \frac{\ell^2}{4R} [A(t) \sin \frac{m\pi x}{L}]^2 + A(t) \sin \frac{m\pi x}{L} \cos \frac{\ell}{R}(y - \tau_K x) \quad (11)$$

where m denotes the number of half waves in the axial direction, ℓ is the number of full waves in the circumferential direction, and τ_K is a skewedness parameter, introduced to account for a possible skewedness of the asymmetric modes. The expression contains one generalized coordinate, $A(t)$, the amplitude of the ‘‘primary’’, ‘‘driven’’ mode. The corresponding model will be referred to as Evensen’s approach [8]. Galerkin’s procedure is applied in order to eliminate the spatial dependence. Using Eq. (11), and applying

the method of averaging to eliminate the time dependence, results in a nonlinear equation for the average vibration amplitude \bar{A} ,

$$(a_{10} - \alpha_{10}\Omega^2)\bar{A} + (a_{31} - \alpha_{31}\Omega^2)\bar{A}^3 + a_{50}\bar{A}^5 = G_{m\ell\tau} \quad (12)$$

where a_{ij} and α_{ij} are constant coefficients depending on the shell properties, imperfection, vibration mode, and applied loading, and where $G_{m\ell\tau}$ is the generalized dynamic excitation. The coefficients are listed in [7]. The normalized frequency parameter Ω is defined by $\Omega = \frac{\omega}{\omega_{lin}}$, where $\omega_{lin} = \sqrt{\frac{a_{10}}{\alpha_{10}}}$ is the small amplitude (“linearized”) frequency for the given parameters. Equation (12) can be used to calculate amplitude-frequency curves for nonlinear single-mode free or forced vibrations of statically loaded, imperfect anisotropic cylindrical shells.

2.2 Extended Analysis

At the second level of modelling, Level-2 Analysis (Extended Analysis), the boundary conditions at the shell edges can be taken into account accurately [4, 6]. A Fourier decomposition of the solution is used in the circumferential direction of the shell, in order to eliminate the dependence on the circumferential coordinate. Subsequently, the resulting boundary value problem for ordinary differential equations in the axial direction is solved numerically by means of the parallel shooting method. A perturbation method is used to assess the influence of large vibration amplitudes, geometric imperfections, and a static deformation on the vibration behaviour [9, 10].

For the static state the following perturbation expansion is assumed:

$$\tilde{W} = \tilde{W}^{(0)} + \xi_s \tilde{W}^{(1)} + \xi_s^2 \tilde{W}^{(2)} + \dots \quad (13)$$

$$\tilde{F} = \tilde{F}^{(0)} + \xi_s \tilde{F}^{(1)} + \xi_s^2 \tilde{F}^{(2)} + \dots \quad (14)$$

where ξ_s is a measure of the displacement amplitude of the static “asymmetric” (non-axisymmetric) mode. In the case of free vibrations, the dynamic lateral excitation is equal to

zero ($\hat{p} = 0$). Considering the case of “single mode” vibrations, i.e. that a single “primary” vibration mode is associated with the (linear) natural frequency ω_c , the following perturbation expansion for the frequency ω is used,

$$\begin{aligned} \left(\frac{\omega}{\omega_c}\right)^2 &= 1 + a_d \xi_v + b_d \xi_v^2 + \dots \\ &+ (b_{110} \xi_t + b_{101} \bar{\xi}) \\ &+ (b_{210} \xi_t + b_{201} \bar{\xi}) \xi_v + \dots \\ &+ (b_{120} \xi_t^2 + b_{111} \xi_t \bar{\xi} + b_{102} \bar{\xi}^2) + \dots \end{aligned} \quad (15)$$

and the corresponding solution is assumed as

$$\begin{aligned} \hat{W} &= \xi_v \hat{W}^{(1)} + \xi_v^2 \hat{W}^{(2)} + \dots \\ &+ \xi_t \xi_v \hat{W}^{(11)} + \xi_t \xi_v^2 \hat{W}^{(12)} + \dots \\ &+ \xi_t^2 \xi_v \hat{W}^{(21)} + \xi_t^2 \xi_v^2 \hat{W}^{(22)} + \dots \\ &+ \dots \end{aligned} \quad (16)$$

$$\begin{aligned} \hat{F} &= \xi_v \hat{F}^{(1)} + \xi_v^2 \hat{F}^{(2)} + \dots \\ &+ \xi_t \xi_v \hat{F}^{(11)} + \xi_t \xi_v^2 \hat{F}^{(12)} + \dots \\ &+ \xi_t^2 \xi_v \hat{F}^{(21)} + \xi_t^2 \xi_v^2 \hat{F}^{(22)} + \dots \\ &+ \dots \end{aligned} \quad (17)$$

In these expansions $\xi_t = \xi_s + \bar{\xi}$, where $\bar{\xi}$ is the amplitude of an “asymmetric” imperfection, and ξ_v is a measure of the displacement amplitude; $\hat{W}^{(1)}$ will be normalized with respect to the shell thickness h and $\hat{W}^{(2)}$ is orthogonal to $\hat{W}^{(1)}$ in an appropriate sense [7]. A formal substitution of these expansions into the nonlinear governing equations for the perfect shell yields a sequence of equations for the functions appearing in the expansions.

The equations governing the first-order dynamic state are given by

$$L_{A^*}(\hat{F}^{(1)}) - L_{B^*}(\hat{W}^{(1)}) = -\frac{1}{R}\hat{W}_{,xx}^{(1)} - \hat{W}_{,yy}^{(1)}(\tilde{W}_{,xx}^{(0)} + h\bar{w}_{0,xx}) \quad (18)$$

$$L_{B^*}(\hat{F}^{(1)}) + L_{D^*}(\hat{W}^{(1)}) = \frac{1}{R}\hat{F}_{,xx}^{(1)} + \tilde{F}_{,xx}^{(0)}\hat{W}_{,yy}^{(1)} - 2\tilde{F}_{,xy}^{(0)}\hat{W}_{,xy}^{(1)} + \tilde{F}_{,yy}^{(0)}\hat{W}_{,xx}^{(1)} + \hat{F}_{,yy}^{(1)}(\tilde{W}_{,xx}^{(0)} + h\bar{w}_{0,xx}) + \hat{p} - \bar{\rho}h\hat{W}_{,tt}^{(1)} \quad (19)$$

Notice that the coefficients of these equations depend on the solution of the fundamental state problem ($\tilde{W}^{(0)}, \tilde{F}^{(0)}$) and initial axisymmetric imperfection $\bar{W} = h\bar{w}_0(x)$. The corresponding equations for the static first-order state ($\tilde{W}^{(1)}, \tilde{F}^{(1)}$) are similar, but do not include the inertia term. The dynamic first-order state equations admit separable solutions of the form

$$\hat{W}^{(1)} = h\{\hat{w}_1(x)\cos n\theta + \hat{w}_2(x)\sin n\theta\}\cos \omega t \quad (20)$$

$$\hat{F}^{(1)} = \frac{ERh^2}{c}\{\hat{f}_1(x)\cos n\theta + \hat{f}_2(x)\sin n\theta\}\cos \omega t \quad (21)$$

where $\theta = y/R$, and n is the number of circumferential waves.

To determine the influence of initial geometric imperfections on the vibration behaviour, the equations of the "imperfect dynamic" second-order state (ξ_v, ξ_t -terms) have to be solved. Details of these equations and the numerical solution procedure can be found in [7].

3 Experimental VCT Results

The investigations performed at the Technion on closely stiffened aluminum shells appeared promising since their low frequency vibration modes, observed in tests, were very similar to their buckling modes [2, 11, 12, 13]. The experimental curves of frequency squared versus axial load of a typical shell, when the test is performed till the buckling of the shell, exhibit a steepening at high loads with a rapid drop in the natural frequency before buckling (see for example Fig. 2

for one of the tested shells, RO-34, [13]). The direct prediction method is essentially a curve fitting to the experimental points, but using those points below 50-60 % of the calculated buckling load, to make it truly nondestructive. The curve fitting becomes easier if the f^2 versus P curve is expressed as:

$$f^2 = (A - BP)^{\frac{2}{q}}, q > 2 \quad (22)$$

where A and B are curve fitted and q is assumed to yield the optimal value. Eq. (22) can be rewritten in another equivalent form

$$f^q = A - BP \quad (23)$$

Equation (22) has the advantage that the curve fitting is now for a straight line.

Another way of directly determining the buckling load using a VCT approach is summarized in the following: Measure the natural frequency at zero load, f_0 . Then measure a few points at low level of applied loads and draw a straight line. Determine the predicted critical value of the load P_{cr} , based on the experimental vibration data, from the following expression:

$$P_{cr} = \frac{f_0^2 P_1}{f_0^2 - f_1^2} \quad (24)$$

where P_1 and f_1 are the coordinates of a point on the straight line. Then plot the curve $(1 - \rho)^2$ versus $(1 - f^{*4})$, where $\rho = \frac{P}{P_{cr}}$ is the ratio of the applied load and the corresponding critical value, and $f^* = \frac{f}{f_0}$.

Another approach is based on the work done at the Technion [2, 11, 12, 13] and consists of finding the real boundary conditions using the VCT method. This approach provides the value of the critical load (P_{sp}), based on the actual boundary conditions. Calculate from the graph the value of the constant ξ and then insert its value in the expression

$$P_{predicted} = P_{cr}(1 - \xi) \quad (25)$$

which yields the actual predicted buckling load. The result of this method is presented in Fig. 3 for the same specimen, shell RO-34, where instead of P_{cr} , the value of P_{sp} is used. One should

note that the predicted buckling load is less than the actual experimental buckling load, yielding a ratio of 0.934, which can be considered as a very good buckling load prediction.

4 Capability of semi-analytical models to support VCT results

The Level-1 Analyses and the Level-2 Analysis have been implemented in FORTRAN programs. One of the stringer-stiffened shells that have been tested earlier at Technion, the RO-34 shell, has been used in the numerical calculations. The (normalized) frequency parameter that will be used in the description of the results is $\bar{\omega} = R\sqrt{(\bar{\rho}h/A_{22})} \omega$ (where A_{22} is an element of the ABD-matrix).

4.1 Simplified Analysis

First, the Simplified Analysis is used. The effect of axial loading on the frequency of the mode corresponding to the lowest natural frequency of the perfect shell (“lowest vibration mode”) will be analysed. The shell is subjected to static axial pre-vibration loading $\lambda = \tilde{N}_0/N_{cl}$, where $N_{cl} = (Eh^2)/(cR)$, $N_0 = -N_x(x = L)$, and $c = \sqrt{3(1 - \nu^2)}$. The variation of the frequency with the loading will be shown up to the load at which the frequency becomes zero.

In Fig. 4 the effect of an imperfection on the load versus frequency curves is illustrated for a specific value of the asymmetric imperfection amplitude ($\bar{\xi}_2 = 0.25$), where the asymmetric imperfection is described by

$$\bar{W}/h = \bar{\xi}_2 \sin \frac{\pi x}{L} \cos \frac{n}{R}(y)$$

In the case of asymmetric imperfections, the behaviour becomes strongly nonlinear when the axial load reaches the limit-point load. It is noted that the effect of axisymmetric imperfections on the frequency is significant also at zero loading [5].

4.2 Extended Analysis

The Simplified Analysis in many cases can reveal the main characteristics of the problem and

is suited for parametric studies. The classical “simply supported” boundary conditions ($N_x = v = W = M_x = 0$) are satisfied only approximately in the Simplified Analysis, and the number of modes that is included in the assumed deflection function might not be sufficient. In the Extended Analysis the boundary conditions are satisfied rigorously, the corresponding ‘secondary’ modes are included, the nonlinear fundamental state is taken into account, and the change of vibration mode during static pre-loading is captured [6].

In Fig. 5 the influence of axial loading on the natural frequencies of the RO-34 shell is shown obtained using the Extended Analysis. The Simplified Analysis (Fig. 4) is able to capture the main trend of the behaviour, but to obtain more accurate results one should use the Extended Analysis.

PREDICTION OF BUCKLING LOADS USING VCT - AN UPGRADED APPROACH

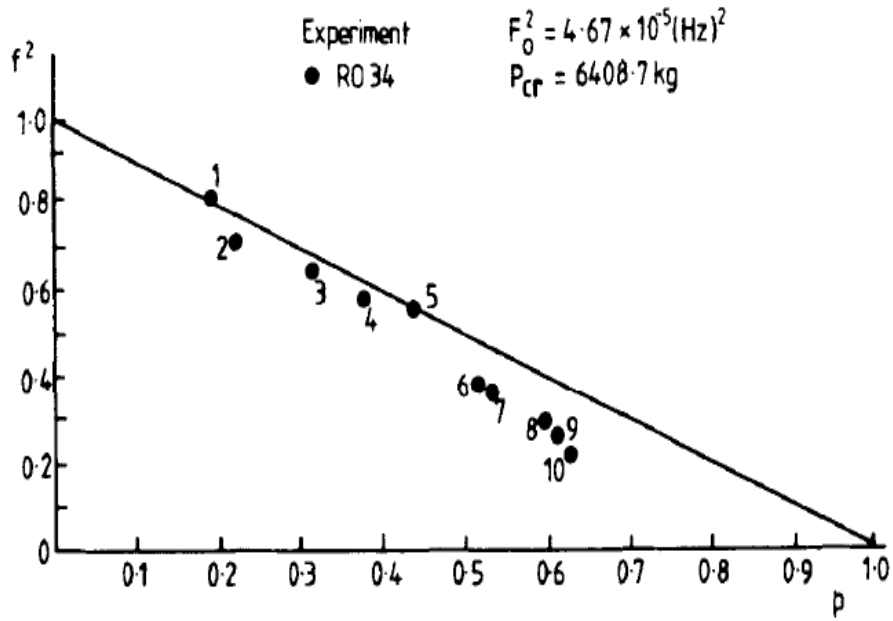


Fig. 2 Technion VCT experiments- frequency squared vs. axial compression for shell RO-34.

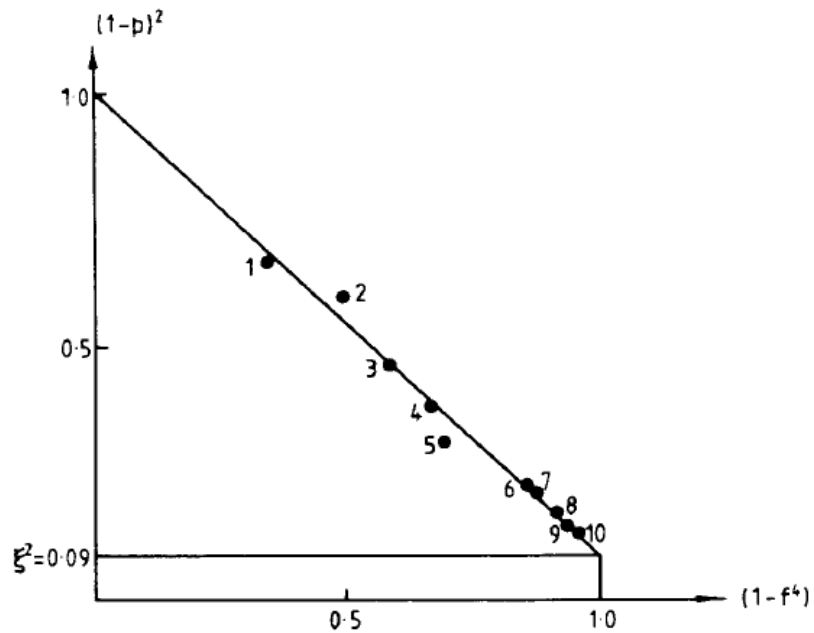


Fig. 3 Empirical method for shell RO-34: $P_{predicted} = 44.86 \text{ kN}$ as compared with $P_{exp} = 42.2 \text{ kN}$.

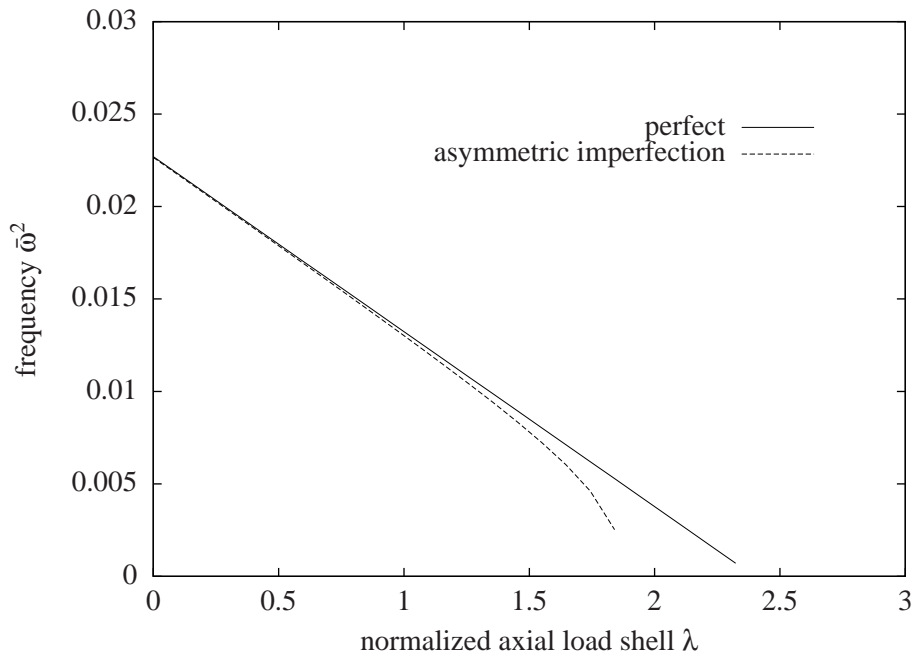


Fig. 4 Effect of axial load on natural frequency of imperfect closely stiffened aluminum shell (RO-34 shell) for lowest vibration mode ($m = 1, \ell = 11$), for perfect shell and for shell with asymmetric imperfection. Simplified Analysis.

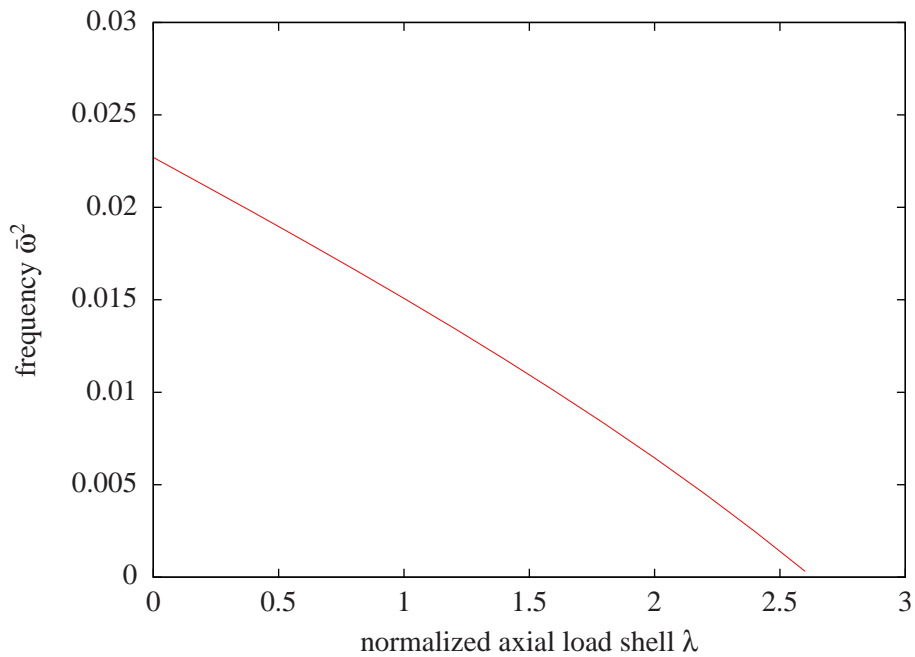


Fig. 5 Effect of axial load on natural frequency of closely stiffened aluminum shell (RO-34 shell). Extended Analysis, SS-3 boundary conditions.

5 Concluding remarks

The availability of a Vibration Correlation Technique (VCT) for nondestructive determination of buckling loads of cylindrical shells has obvious advantages. Two semi-analytical models with different levels of complexity have been presented. In the two approaches employed, both the nonlinear effect of the static state and the nonlinear effect of the geometric imperfections are represented. In this paper, the capability of these analysis tools, which can be used to improve the VCT, is illustrated. Application of these tools gives the possibility for an extension of the existing semi-empirical Vibration Correlation Technique for shells, to a VCT in which vibration measurements and analysis tools are combined.

6 Contact Author Email Address

Corresponding author: e.jansen@isd.uni-hannover.de

References

- [1] M.A. Souza, W.C. Fok, and A.C. Walker. Review of experimental techniques for thin-walled structures liable to buckling, Part I-Neutral and unstable buckling. *Experimental Techniques*, 7:21–25, 1983.
- [2] J. Singer, J. Arbocz, and T. Weller. *Buckling Experiments: Experimental Methods in Buckling of Thin Walled Structures. Shells, Built-up Structures, Composites and Additional Topics-Volume 2*. John Wiley & Sons, Inc., New York, 2002.
- [3] E. L. Jansen. A comparison of analytical-numerical models for nonlinear vibrations of cylindrical shells. *Computers & Structures*, 82:2647–2658, 2004.
- [4] E. L. Jansen. A perturbation method for nonlinear vibrations of imperfect structures: Application to cylindrical shell vibrations. *International Journal of Solids and Structures*, 45:1124–1145, 2008.
- [5] E. L. Jansen. The effect of geometric imperfections on the vibrations of anisotropic cylindrical shells. *Thin-Walled Structures*, 45:274–282, 2007.
- [6] E. L. Jansen. Effect of boundary conditions on nonlinear vibration and flutter of laminated cylindrical shells. *Journal of Vibration and Acoustics*, 130:011003–1 – 011003–8, 2008.
- [7] E. L. Jansen. *Nonlinear Vibrations of Anisotropic Cylindrical Shells*. PhD thesis, Faculty of Aerospace Engineering, Delft University of Technology, The Netherlands, 2001.
- [8] D. A. Evensen. Nonlinear Flexural Vibrations of Thin-Walled Circular Cylinders. NASA TN D-4090, 1967.
- [9] L.W. Rehfield. Nonlinear free vibrations of elastic structures. *Int. J. Solids Structures*, 9:581–590, 1973.
- [10] J. Wedel-Heinen. Vibrations of Geometrically Imperfect Beam and Shell Structures. *Int. J. Solids Structures*, 27(1):29–47, 1991.
- [11] H. Abramovich, J. Singer, and A. Grunwald. A nondestructive determination of Interaction curves for buckling of stiffened shells. Report TAE-341, Dept. of Aeronautical Engineering, Technion, I.I.T., Haifa, Israel, 1981.
- [12] T. Weller, H. Abramovich, and J. Singer. Correlation between vibrations and buckling of cylindrical shells stiffened by spot-welded and riveted stringers. Report TAE-537, Dept. of Aeronautical Engineering, Technion, I.I.T., Haifa, Israel, 1985.
- [13] Y. Segal. *Prediction of buckling load and loading conditions of stiffened shells from vibration tests*. M.Sc. Thesis (in Hebrew), Faculty of Aeronautical Engineering, Technion, I.I.T., Haifa, Israel, 1980.

Copyright Statement

The authors confirm that they, and/or their company or organization, hold copyright on all of the original material included in this paper. The authors also confirm that they have obtained permission, from the copyright holder of any third party material included in this paper, to publish it as part of their paper. The authors confirm that they give permission, or have obtained permission from the copyright holder of this paper, for the publication and distribution of this paper as part of the ICAS 2014 proceedings or as individual off-prints from the proceedings.